PHYSICAL REVIEW A VOLUME 8, NUMBER 3 SEPTEMBER 1973

Clustering of Ar to Li^+ and a Comparison of Drift-Tube Models

G. E. Keller, R. A. Beyer,* and L. M. Colonna-Romano

U. S. Army Ballistic Research Laboratories, Aberdeen Proving Ground, Maryland 21005

(Received 9 April 1973)

The clustering of Ar to Li^+ has been studied experimentally using a drift tube. The measurements were made at a gas temperature of 319 °K. The gas pressure was varied between 0.5 and 1.5 Torr, and E/N was varied between 9 and 24 Td ($1 \text{ Td} = 10^{-17} \text{V cm}^2$). Under these conditions, the major reaction is $Li^+ + Ar + Ar \rightleftharpoons Li^+(Ar) + Ar$. The rate coefficients and the mobility of $Li^+(Ar)$ were deduced by comparing measured arrival-time profiles of the ions with profiles generated by a three-dimensional, numerical drift-tube model. The predictions of this model are compared in some detail with those of two analytical, three-dimensional, drift-tube models. In all cases the agreement is satisfactory. We find that the association-rate coefficient k_1 is 1.8×10^{-31} cm^6/sec and remains constant over the range of E/N used and that the collisional-dissociation-rate coeffiecient k_{-1} increases from 2.0×10^{-13} cm^3/sec at $E/N = 9$ Td to 3.2×10^{-13} cm^3/sec at $E/N = 24$ Td. In addition, we find the reduced mobility of $Li^+(Ar)$ in Ar to be 2.0 $\text{cm}^2/\text{V sec}$, measured at 319 °K. The amounts by which these values may be in error were determined as $\pm 24\%$ for the association-rate coefficients, $\pm 22\%$ for the collisional-dissociation-rate coefficients, and $\pm 16\%$ for the mobility of $Li^+(Ar)$. The mobilities of K^+ in N_2 and of K^+ in Ar were determined during checks for systematic errors in the new drift tube. The mobility of Li^+ in Ar was also determined in the course of this work. Both random and systematic errors were considered in the determination of the standard deviations of these measurements. These reduced mobilities and their standard deviations are: K^+ in N_2, 2.55 ± 0.06 $\text{cm}^2/\text{V sec}$, measured at 310 °K; K^+ in Ar, 2.73 ± 0.06 $\text{cm}^2/\text{V sec}$, measured at 310 °K; and Li^+ in Ar, 4.57 ± 0.12 $\text{cm}^2/\text{V sec}$, measured at 319 °K.

I. INTRODUCTION

In 1965 Narcisi and Bailey found several metallic positive ions in the earth's upper atmosphere.[1] Since that time there have been speculations about the effect of the clustering of neutral atmospheric gases to the atomic metallic ions, specifically in regard to the number densities of the metal ions and metal atoms.[2] A discussion of the effect of CO_2 clustering to Na^+ ions at 95 km has been published elsewhere.[3]

This paper reports some of the initial experimental results obtained with a new drift-tube facility at the Ballistic Research Laboratories. As a check for gross systematic errors in the new equipment, the mobility of K^+ ions in N_2 was compared with previous measurements.[4,5] In addition, the mobilities of K^+ in Ar, Li^+ in Ar, and $Li^+(Ar)$ in Ar were measured.

The clustering of Ar to Li^+ and the collisional dissociation of the cluster ion was chosen for intensive study. This reversible reaction can be written as

$$Li^+ + Ar + Ar \underset{k_{-1}}{\overset{k_1}{\rightleftharpoons}} Li^+(Ar) + Ar \,, \tag{1}$$

where the parentheses around Ar in the notation for the cluster ion indicate that the original ion was Li^+. There are several reasons for the study of this reaction. The first, and most important, is that while we had established that other gases cluster to Li^+ faster than Ar,[6] Ar clusters just fast enough that under our experimental conditions Li^+ and $Li^+(Ar)$ are the major ions *and* the arrival profiles of the two ions are noticeably different, implying that chemical equilibrium has not been established. Secondly, Ar is often used as a buffer gas in swarm experiments because it is assumed that it does not react. It has been shown that clustering of the buffer gas with ions under study can be important.[7] Hence, means for establishing how much the buffer gas may be participating in the reaction process under study are needed. Finally, Ar clustering to Li^+ is a very simple form of clustering in which electrostatic forces predominate.[8]

In our early drift-tube measurements[3] we analyzed the drift-tube data by comparing measured total current ratios of the ions involved. Because that method assumes equal detection sensitivities for the various ions, we chose to deduce the rate coefficients for reaction (1) by comparing the measured arrival-time profiles of the two ions with predicted profiles generated by the drift-tube model due to Kregel. (A description of the model is available in a report by Keller *et al.*[9]) This model is extensively compared with two other three-dimensional drift-tube models[10,11] to establish their agreement and to choose the most appropriate model for the predictions desired.

The suggestion has been made[12] that the units of E/N be denoted by the "townsend," or Td, where $1 \text{ Td} = 10^{-17} \text{ V cm}^2$. This designation will be used throughout this paper. All mobilities quoted in this paper are reduced to 0 °C and 760 Torr.

II. APPARATUS AND EXPERIMENTAL PROCEDURE

The drift tube is an all-metal, bakable tube which can be used with drift lengths up to 44 cm. For the work described in this paper, the tube has been operated in two configurations. The drift length of the tube in configuration I (Fig. 1) is 44 cm, while it is 7.48 cm in configuration II (Fig. 2). Oil diffusion pumps with water-cooled chevron baffles and zeolite traps were used throughout. All chambers have been pumped to 2×10^{-9} Torr by use of a 48-h 200 °C bake. The drift-tube pressure at the start of a day is typically 5×10^{-9} Torr, and rises to an equilibrium value of about 1×10^{-7} Torr in a few hours if the 4-in. diffusion pump is valved off and no gas is added to the tube.

Two sources of ions are used in this work, one to produce K^+ and the other Li^+. The source of K^+ ions is a platinum gauze filament coated with Kingman feldspar.[13] This material emits K^+ in copious quantities. In addition, Rb^+ is emitted in a much smaller amount. The source of Li^+ ions is a platinum gauze filament coated with β-eucryptite enriched in the mass 7 isotope.[13] Resistive heating of the filament is provided by a current-controlled low-voltage dc power supply. The ionic source is operated at a low output current to minimize space-charge effects in the drift region.

Both configurations of the drift tube use 20-cm-i.d. drift hoops whose electrical (but not mechanical) design is patterned after that of Crompton *et al.*[14] and Albritton *et al.*[15] Only high-purity alumina and Supramica (Mycalex Corp. of America) were used as insulators for drift-hoop mounting and all other insulation in the drift tube. In configuration I, there are three ion shutters. They are constructed of parallel stainless-steel wires spot welded to flat rings. The wires have a spacing of about 1.6 mm; a gate is formed by two grids spaced 3.2 mm apart. In configuration II, there are two ion shutters. One is formed by two wire grids, as before. The other is formed by a wire grid and the end plate of the drift tube, which are 3.2 mm apart. In either configuration the source is run continuously. One of the gates is electrically biased to inhibit the drift of the ions. Then this bias is momentarily reversed, which permits a small group of ions to drift down the tube from the chosen gate.

The end plate of the drift tube is electrically insulated from ground so that the current to it can be measured and, if desired, a small potential may be applied. For all the work reported here, the end plate was grounded. The exit aperture is 0.4 mm in diameter. As shown in Figs. 1 and 2, differential pumping is used to reduce the pressure in the mass spectrometer section. When the Ar pressure in the drift tube is 2 Torr, an ion gauge in the mass-spectrometer chamber reads 5×10^{-5} Torr. For pressures higher than these, we have observed a decrease in the signal of the weakly bound cluster ions, presumably due to breakup of these ions in either the first differential pumping chamber or the mass-spectrometer chamber. The skimmer between these chambers has a 4.3-mm-diam. orifice in its tip and is mounted about 3 cm from the exit aperture. It is both electrically insulated from ground and removable. The skimmer is normally operated at a potential of a few volts below ground. After the ions pass through the skimmer into the low-pressure region of the mass-spectrometer chamber, they are further accelerated and focused. As will be discussed later, the skimmer has been found to contribute to a difference in the sampling efficiency of this system for ions of different mass.

The mass spectrometer is a monopole rf spec-

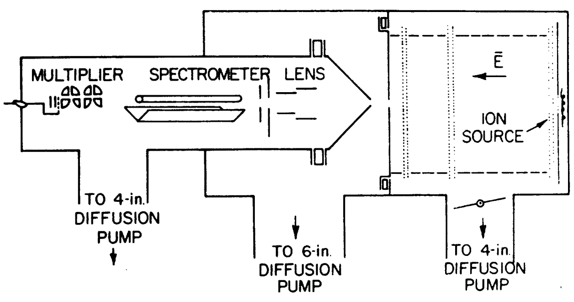

FIG. 1. Drift-tube configuration I.

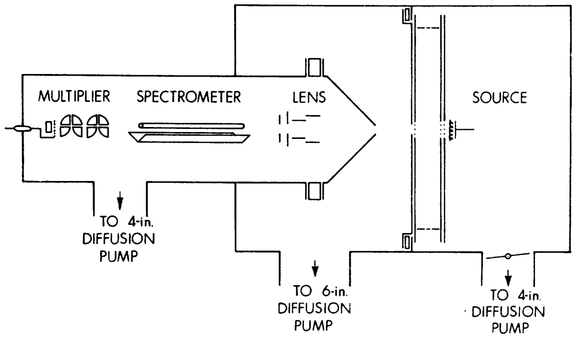

FIG. 2. Drift-tube configuration II.

trometer modified to operate with either positive or negative ions created at ground potential. The spectrometer has better than unit resolution to several hundred amu. The ions are detected by a 16-stage Ag-Mg multiplier operated in a pulse-counting mode. These output pulses pass through a preamplifier, amplifier, and discriminator to both a counter and a 1024-channel time-of-flight analyzer.

The stainless-steel gas feed line between the regulator and the drift tube has both a large reservoir tank and a U-tube trap. Enough gas for a week's operations was admitted to the feed line at one time; the trap was allowed to cleanse this gas sample at least overnight before the gas was used. This trap, maintained at a temperature of about -100 °C,[16] removed water and other impurities very effectively.

The gas pressure in the tube is measured by a MKS Baratron bakable capacitance manometer and a Datametrics Barocel bakable capacitance manometer. These two manometers agree quite well over the pressure range that has been used, 50 mTorr to 2 Torr. The reading of the MKS instrument has always been just about 2% higher than that of the Datametrics instrument; the maximum fluctuation of their difference is 1 mTorr/day. The output of the Datametrics manometer is fed through a control circuit to a servodriven variable leak valve so that the gas pressure can be regulated at any fixed value to within 0.3 mTorr.

In configuration I, four iron-constantan thermocouples were used to monitor the gas temperature along the outside of the drift space. The thermocouple leads pass into the vacuum system through iron-constantan wires brazed into an ultrahigh-vacuum tube-type feed-through. Tests were made to determine whether the thermocouples had to be firmly attached to large stainless-steel plates or whether they could be firmly attached to insulator blocks on the drift-hoop string. Both types of connections gave the same temperature; the latter type of connection was used in this work. Measurements on all of the four thermocouples in the drift tube at the time of these tests showed that the gas just a few centimeters from the source was at the same temperature as that 40 cm away, so that, except for a steep gradient in gas temperature which must exist in the immediate vicinity of the hot filament, we assume that the ions drift through a gas of constant temperature. At first, the temperature readout was made using an ice bath and a sensitive electrometer. During the K^+ mobility measurements, a sensitive pyrometer (API Instruments Co.) was installed. Its indicating range is -15 to 65 °C, and its advertised accuracy is ±2% of its span, or ±1.6 °C. The two readout methods gave no measureable differences in temperature. We found that at least 4 h of warmup were required for the gas and drift tube to reach a stable temperature so that reproducible data could be taken. In configuration II, one thermocouple was used, due to the short drift distance.

Potentials for the drift hoops were furnished from a resistor string outside the vacuum system. The applied drift field was monitored with a Fluke Model No. 8100A digital multimeter, whose long-term accuracy is claimed to be better than ±0.1%.

TABLE I. Boundary conditions of drift-tube models.

	Source axial shape	Source radial shape	Finite drift-tube radius	Detector type	Detector extent
Kregel model	Gaussian, specified width[a]	Gaussian, specified width[a]	Possible, but not usually included	Transmitting	Pinhole
Gatland model	δ function	Uniform, specified width	No	Transmitting	Pinhole
Woo-Whealton model	Uniform, specified width	1. Bessel function, diameter of drift tube. 2. Uniform, diameter of drift tube. 3. Uniform, diameter smaller than drift-tube diameter.	Yes, walls assumed perfectly absorbing	Transmitting	Circular aperture, specified size

[a] Essentially arbitrary, shape listed is shape usually used.

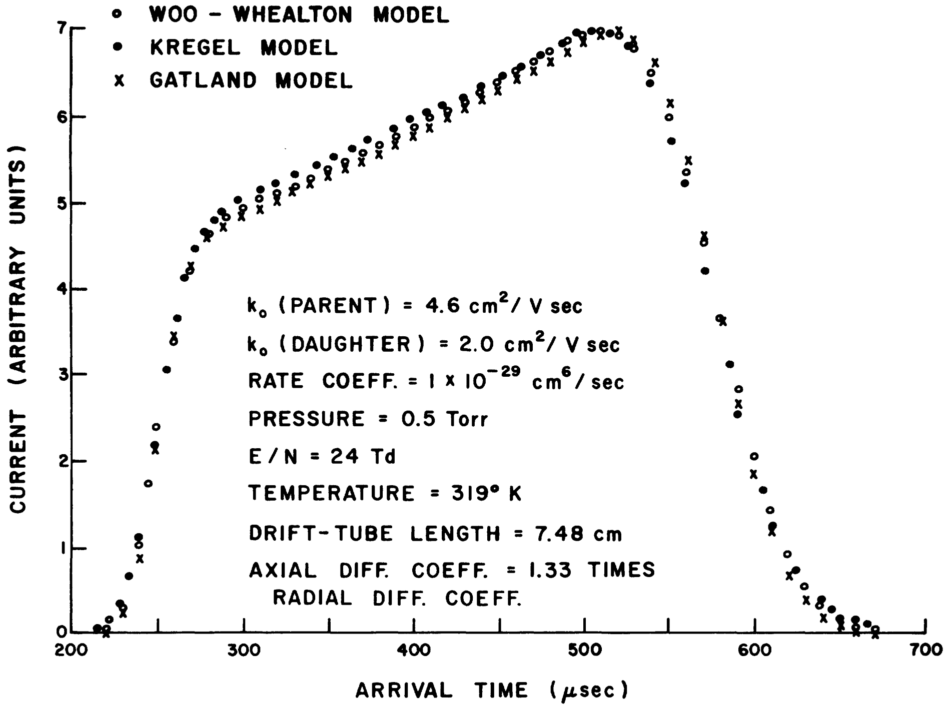

FIG. 3. Comparison of daughter-ion arrival curves calculated using three different drift-tube models. The parameters are hypothetical and are chosen to illustrate the effects of a fast three-body reaction.

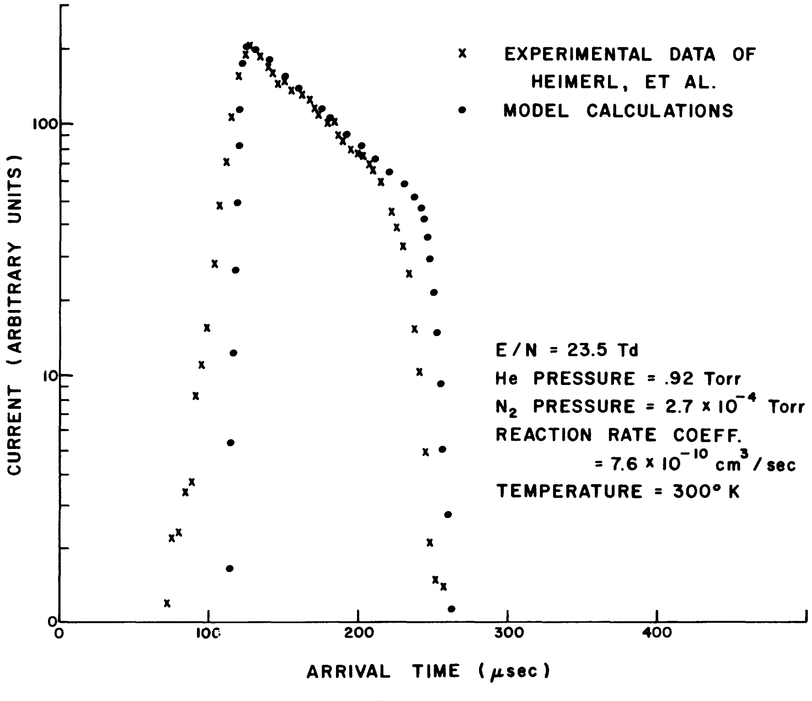

FIG. 4. Comparison of experimental data with drift-tube-model predictions. Arrival spectra for N$^+$ in He.

III. DRIFT-TUBE MODELS

In this section we discuss and compare three three-dimensional drift-tube models. The first is that due to Woo and Whealton,[10] who solved analytically the transport equations for the case of two ions with one depleting reaction. The second is due to Gatland,[11] who also solved the transport equations analytically, but for two ions with two interconverting reactions. The third is due to Kregel,[9] whose approach to the solution of the transport equations is numerical. Kregel's model presently treats at most three ions with six possible interconverting reactions, but it could be made to handle any number of ions and reactions. Our Li^+-in-Ar data were reduced using Kregel's model.

There were several motivations for the development of a numerical drift-tube model. The primary one was the desire to be able to generate the arrival profiles for more than two ions linked by more than one or two reactions. Further, a numerical model makes it possible to model different source conditions and/or different boundary conditions. Finally, a numerical model makes it possible (although difficult) to study special effects, such as the study of back diffusion to an absorbing source shutter which is discussed later in this paper.

While Woo and Whealton[10] and Gatland[11] arrived at analytical solutions to the transport equations, Kregel's model is a numerical simulation of the actual transit of the ions in a drift tube. The program follows the progress of the ion swarms as they drift, diffuse, and interconvert with time. After several hundred small time steps the ions have traveled the length of the drift tube. The currents due to the charged particles are calculated as the number density distributions traverse the end of the drift tube.

The three models also differ in the boundary conditions each applies. These conditions are compared in Table I. The table reflects the geometries for which the details are furnished in the references. Each of the models permits the axial and radial diffusion coefficients for the ions to be independent, so that they are not limited to low E/N.

We have compared the three models for a number of particular cases. The first comparison is shown in Fig. 3. We consider the small differences in the model predictions quite satisfying, considering the inherent differences in the models.

Having found that the models all predict very similar hypothetical profiles, one might ask if the models predict physically realistic profiles. In particular, given two measured mobilities and a rate coefficient established by measurements in drift tubes and in other experiments, we sought

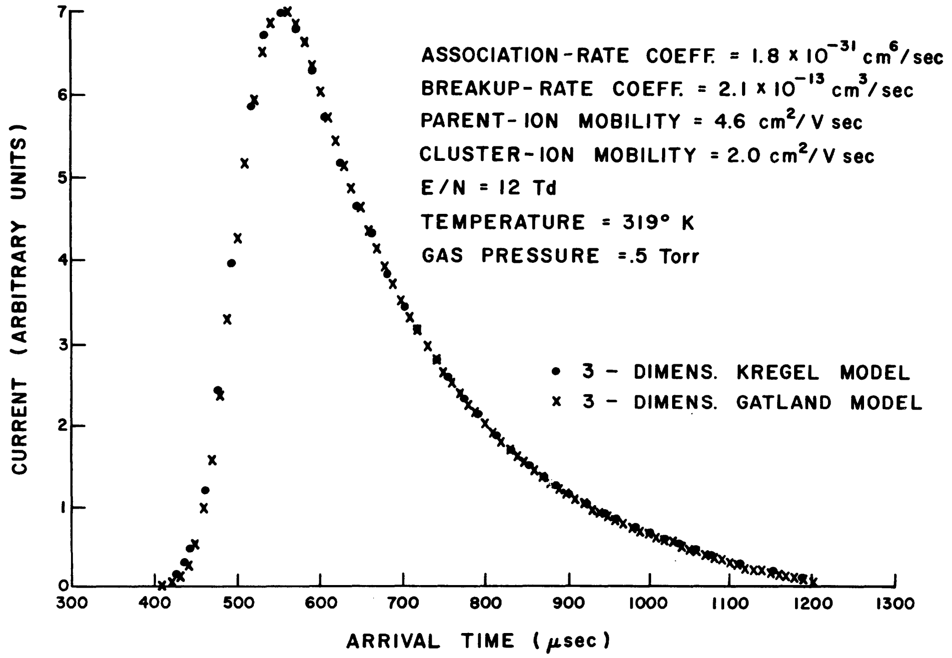

FIG. 5. Comparison of cluster-ion arrival profiles calculated using Kregel model and Gatland model. The parameters chosen are appropriate for Li^+ (Ar) in Ar.

to demonstrate that the models predict arrival-time profiles which resemble measured profiles. This demonstration is illustrated by Fig. 4. We took the reported experimental and deduced parameters from Heimerl *et al.*[17] and attempted to duplicate their published data. Figure 4 shows the experimental profile of N^+ ions produced by the $He^+ + N_2$ reaction and calculations of Kregel's model. The longitudinal diffusion coefficient used in the calculations was arbitrarily 15% greater than the Einstein value. The profiles generated by the three models fell right on top of each other, so that only one profile was plotted. We could not resist the temptation to see how well the data could be fit; we found that an excellent fit to the top slope and the entire trailing edge of the data could be obtained by increasing the reaction rate coefficient about 10% over Heimerl's value, increasing the mobility of He^+ in He by 7%, and using a value of the longitudinal diffusion coefficient about twice the Einstein value.

The Kregel model was further compared with the Gatland model for a case involving two ions and two interconverting reactions. One such comparison of the expected cluster-ion arrival profiles is shown in Fig. 5. The case chosen is not arbitrary; the conditions are close to the final results of this paper for Li^+ drifting in Ar. The curve shown is the expected profile for $Li^+(Ar)$. In the case of curves for Li^+, the Gatland curves are slightly narrower than the Kregel predictions due to the δ-function source of the former model. Predicted current ratios $Li^+/Li^+(Ar)$ differ by less than 5% between the two models.

Edelson[18] has shown that if the source pulse has finite radial extent and the detector is a pinhole, drift-tube experiments can usually be treated as one-dimensional problems. We found that this is certainly true for the conditions of these measurements. A comparison of the Kregel model with and without radial diffusion is shown in Fig. 6.

Lowke[19] calls attention to the fact that just after the ions have passed through the source shutter of a drift tube and the shutter is electrically closed, back diffusion of the ions into the absorbing source shutter may significantly alter the arrival-time profiles of the ions which arrive at the end plate of the drift tube. This sort of question can be addressed with a numerical model, and we calculated the effect it might have on our results. We did this by depleting the ion densities by a fixed fraction each time step if they were calculated to be separated from the drift space by the source shutter. We adjusted the fraction so that the ensuing, simulated Li^+ arrival profile was depleted by about 25% in area. The resulting Li^+ arrival profile was unchanged in shape and was shifted in time less than 0.5%. The $Li^+(Ar)$ arrival profiles

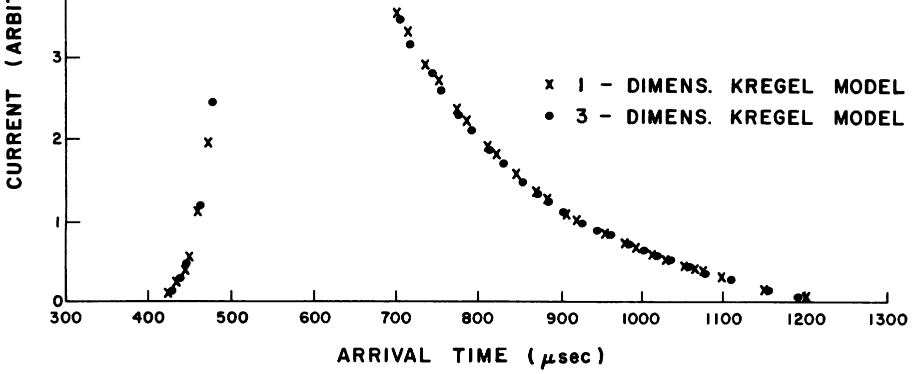

FIG. 6. Comparison of cluster-ion arrival profiles calculated using three-dimensional Kregel model and one-dimensional Kregel model. The parameters chosen are appropriate for $Li^+(Ar)$ in Ar.

with and without the back diffusion effects discussed by Lowke are shown in Fig. 7. We see that our present work was unaffected by this effect.

We have examined the effect that an absorbing end plate might have on our results using two different models. We applied the Woo-Whealton model to two very different cases.[20] We examined cases for which the ion velocities were slower, E/N lower, and the gas pressure smaller than any that we used for the work reported here, where the ratio of drift velocity to diffusion coefficient, v/D, should be smallest and thus an effect from an absorbing end plate should be greatest. In fact, we found a small (0.2% or less) change in the mobility that would have been deduced from the arrival time of the peak, but no change whatsoever in the shape of the parent-ion peak. That is to say, the whole peak shifted very slightly toward shorter times, but the shape of the profile remained the same. Kregel[21] developed a numerical code which takes any arbitrary ionic number density distribution and computes from it the current that would be measured when the ions impact either a transmitting or absorbing end plate. We applied this code to several different cases. Again, while the whole of the arrival time peak is shifted to earlier times, the percentage change of the arrival time was very small and the current profiles for an absorbing or transmitting end plate were identical. We conclude that one cannot, by demonstrating a remarkable fit of data to the predicted shape of an arrival curve, determine which model of the end plate is most nearly correct for the experiment. We also conclude that the transmitting models, which are much easier to manipulate, are sufficiently correct to be used for the reduction of any of our experimental data.

IV. RESULTS

A. K^+ in N_2 and Ar

The tube was operated in configuration I for initial checks and for the mobility measurements involving K^+ ions. The transport of K^+ in N_2 was used for all initial checking of the system, for, under the conditions of this investigation, the ratio of the measured total currents of $K^+(N_2)$ to K^+ was always less than 0.02. Assuming no mass discrimination in the sampling process, the K^+ ions were clustered less than 2% of the time they drifted down the tube.

For the measurement of mobilities, a master clock was used both to pulse open an ion shutter and to start the multichannel analyzer operated in the time-of-flight mode. This process was repeated until an oscilloscope display of the analyzer contents showed that the arrival-time spectrum for the ion was well established.

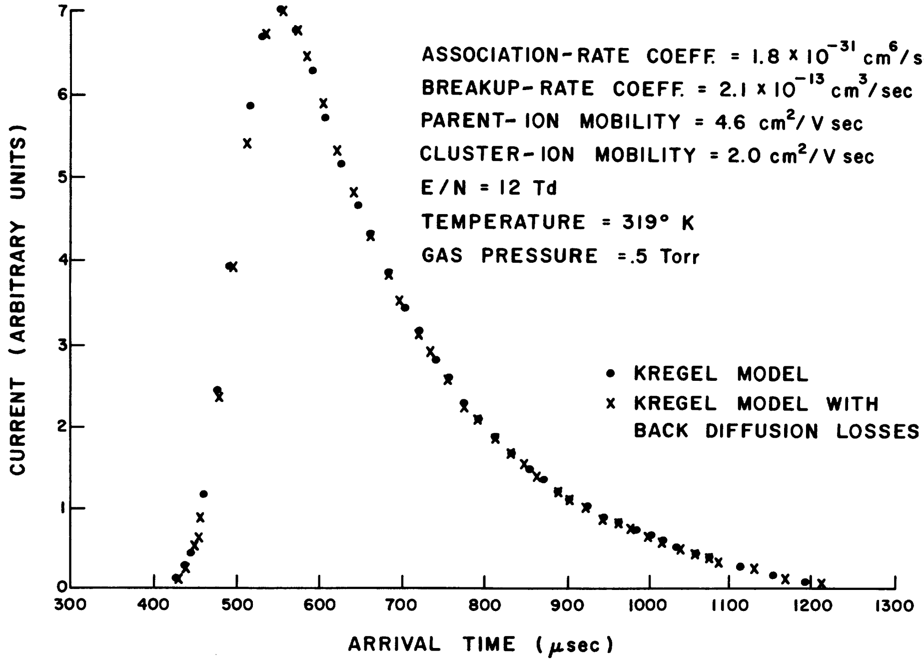

FIG. 7. Comparison of cluster-ion arrival profiles calculated using Kregel model and Kregel model with back diffusion losses. The parameters chosen are appropriate for Li^+ (Ar) in Ar.

We sought to find evidence for ion-ion interactions resulting from excessive ion densities in the source region. We did this by increasing the source current in steps and examining the width of the arrival profile for K$^+$. We found that indeed the peak began to broaden as the source current increased. We took all our data with a source current well below the value where peak broadening could be observed. For this source current, the signal rate rarely exceeded 0.1 ion per pulse, so that effects from dead time in the multichannel analyzer do not affect our results.

Arrival spectra were obtained using each ion shutter in turn as the "source." Since the distance between the shutters was known, the three spectra could be used to infer an ion mobility free from the end effects of either ion source or detector. Mobility data were taken for gas pressures of 0.5 to 1.5 Torr. The zero-field reduced mobility of K$^+$ in N$_2$ was found to be 2.55 cm^2/V sec and that of K$^+$ in Ar was found to be 2.73 cm^2/V sec. Both measurements were made at 310 °K.

B. Li$^+$ in Ar

The drift tube was operated in configuration II for the studies of Ar clustering to Li$^+$. A preliminary report of these studies has been given.[22] All measurements were made at 319 °K, somewhat above room temperature due to the heating of the gas and tube by the Li$^+$ source. Measurements were made at pressures of 0.5, 1.0, and 1.5 Torr, and E/N was varied between 9 and 24 Td. Under these conditions, reaction (1) was the major reaction. We used arrival-time profiles for the Li$^+$ and Li$^+$(Ar) ions at each pressure and E/N to deduce the E/N dependence of both mobilities, the rate coefficients of both reactions, and an estimate of the axial diffusion coefficient for Li$^+$ in Ar. Comparison with measured current ratios also yielded an estimate of the difference of detection sensitivities for our system for the two ions at $E/N = 12$ Td and at $E/N = 24$ Td.

Typical arrival-time profiles for Li$^+$ in Ar and Li$^+$ (Ar) in Ar are shown in Figs. 8 and 9, respectively. The Li$^+$ arrival profile has the expected skewed Gaussian shape plus a contribution at late times from ions which emerged from the tube unclustered but had spent some time as the slower cluster ions. We used the mean arrival time of the skewed Gaussian portion of these profiles to determine the mobility of Li$^+$ in Ar. The value was found to be 4.57 cm^2/V sec and was independent of E/N.

The remaining physical parameters were deduced by comparing measured arrival-time curves with curves calculated using Kregel's model for a variety of parameters to ensure that the desired physical quantities were uniquely determined. We required a good fit of arrival curves for both ions at at least two pressures, usually 0.5 and 1.5 Torr. The parameter that resulted in a best fit of all four curves did not result in a best fit of each of the four curves simultaneously. Figure 9 illustrates this point. $k_1 = 1.9\times 10^{-31}$ cm^6/sec and $k_{-1} = 2.2\times 10^{-13}$ cm^3/sec resulted in a best fit for the four curves; Fig. 9 shows how closely the profile for Li$^+$(Ar) at 1.5 Torr and $E/N = 12$ Td is fit. This figure is taken directly from the computer output for the $E/N = 12$ Td data analysis. The computer printed the symbol E for the experimentally measured data points, T for the points calculated from the model, and D for any overlapping points. Plots such as this greatly simplified the selection of appropriate rate coefficients and other parameters.

At all values of E/N, the best value of the mobility of Li$^+$(Ar) was found to be 2.0 V cm^2 at 319 °K. The accuracy of this determination clearly

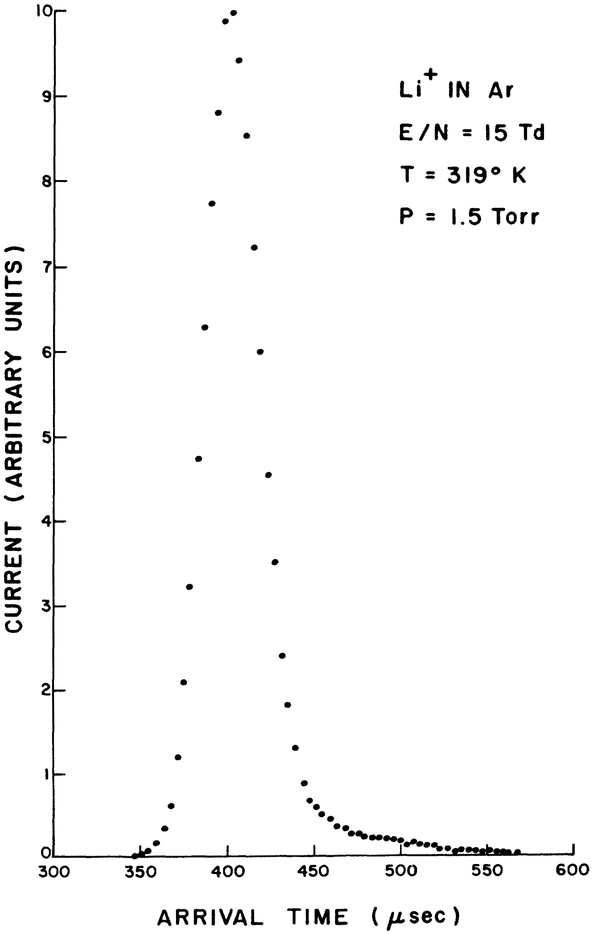

FIG. 8. Typical experimental Li$^+$ current profile.

rests on the accuracy of the previous determination of the mobility of Li^+.

The three-body association- (or "clustering") rate coefficient k_1 as a function of E/N is shown in Fig. 10. At these low values of E/N, this rate coefficient is found to be constant. The error bars shown on the figure indicate the maximum possible error, random and systematic, which may be associated with the determination of the rate coefficient. These errors will be discussed in Sec. IV C.

The two-body collisional-dissociation-rate coefficient k_{-1} as a function of E/N is shown in Fig. 11. Even at these low values of E/N, this rate coefficient is sensitive to small changes in E/N, or equivalently the ion energy. The meaning of the error bars is the same as for those on Fig. 10.

The work of Wannier,[23] as put into a more convenient form by McDaniel and Moseley[24] and by Thomson *et al.*,[25] led us to expect that both the axial and the radial diffusion coefficients for Li^+ in Ar might increase from the Einstein value in our range of E/N values. Unfortunately, we cannot measure the radial diffusion coefficient. To have made a *bona fide* measurement of the axial diffusion coefficient would have required us to use an initial burst of ions whose axial dimension approached zero, which, for our experiment, lowers the ion count rate to unacceptably low levels. Nevertheless, we obtained an estimate of the E/N dependence of the axial diffusion coefficient by the following method. We set the source pulse to just that width which should produce an initial burst of Li^+ ions whose axial length was 0.3 cm. With the initial width in the numerical drift-tube model set to 0.3 cm, we deduced from the width of the measured Li^+ profile the multiplicative factor by which the axial diffusion coefficient exceeds the Einstein value of the diffusion coefficient. The results of this study are shown in Fig. 12, which shows that the axial diffusion coefficient for Li^+ in Ar does indeed seem to be strongly dependent on E/N in the range considered. Error bars are not given for these estimated values. Also included on Fig. 12 are the factors that Wannier's polarization model predicts. We find the comparison very satisfying, considering the manner by which we obtained our estimates.

A drift-tube-model calculation yields not only arrival-time profiles for the ions, but also the correct ratio of the currents of the ions to the

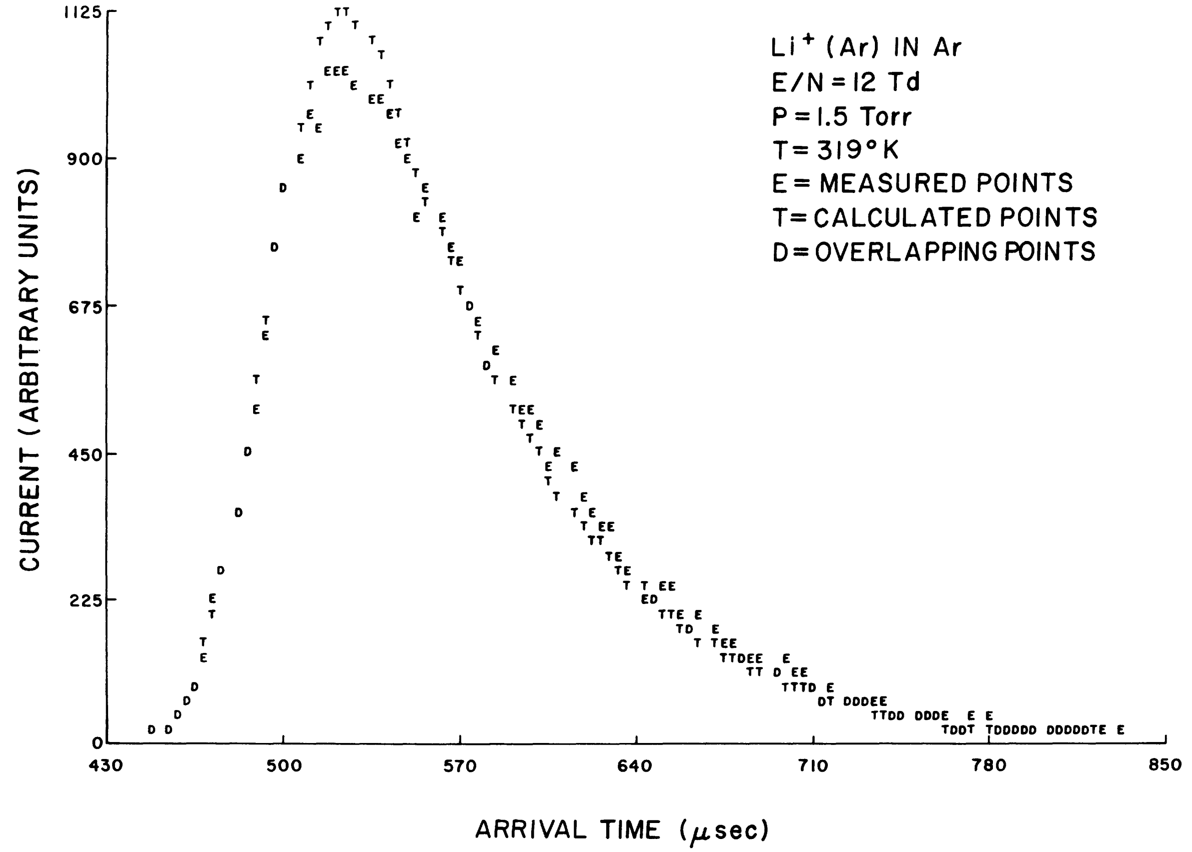

FIG. 9. Typical comparison of experimental data with model calculations.

orifice in the end plate of the drift tube. Accordingly, we compared measured current ratios of the two ions with the current ratios predicted from the best-fitting calculated profiles at $E/N = 12$ Td and $E/N = 24$ Td. We were surprised to find that the measured ratio of Li^+ to $Li^+(Ar)$ was a factor of 8 to 10 lower than the calculated ratio at $E/N = 12$ Td, and a factor of 5 to 10 lower at $E/N = 24$ Td. McKnight[26] has made a measurement of the current ratio of Li^+ to $Li^+(Ar)$ with his drift tube which agrees quite well (within a factor of 2) with that predicted by our model calculations. We noted that the separation of McKnight's differentially pumped sampling chambers is accomplished with a relatively flat aperture, while our chambers are separated by a conical "skimmer." Thus, we performed a brief series of tests at $E/N = 12$ Td to determine whether our skimmer led to errors in the measured current ratio. First, the exit orifice was reduced to 0.2-mm diameter and the current ratio was measured to be a factor of 8 to 10 lower than the calculated (and assumed correct) ratio. Second, the skimmer was removed and the current ratio was measured to be only 60% to 80% low. (An error of this amount is reasonable for a particle multiplier operated at our relatively low voltage.) Third, the (well-cleaned) skimmer and the 0.4-mm-diam. exit orifice were replaced and the measured current ratio was again a factor of 8 to 10 low. The final test was to append a blunt front end to the skimmer. Ions emerging from the exit orifice then saw a flat plate with an orifice, but once through the skimmer orifice, conditions were unchanged. Under these circumstances, the measured current ratio was still a factor of 8 to 10 lower than the calculated ratio. We conclude that some aspect of the transit of the ions through the conical skimmer after they have passed through its orifice discriminates against Li^+ relative to $Li^+(Ar)$. We plan to modify our drift tube so that it can operate efficiently without a skimmer.

C. Discussion of Errors

Errors in the determination of the gas pressure, the gas temperature, the drift distance, the drift voltage, and the drift time could cause errors in our determinations of mobilities and rate coefficients.

We estimated the possible systematic errors as follows: The use of two different pressure manometers should minimize errors due to incorrect pressure determinations. Furthermore, the agreement of the mobility of K^+ in N_2 with previous determinations[4,5] adds confidence in the pressure (and temperature) measurement. Nevertheless, a possible error of ±2% seems appropriate for the pressure measurement. Having compared our pyrometer against a combination of thermocouple, ice bath and electrometer, we consider a possible error of ±1% appropriate for the temperature measurement. In addition, we have allowed for an error of ±0.2 V in the measurement of the potential across the drift space, ±0.5 mm in measurements

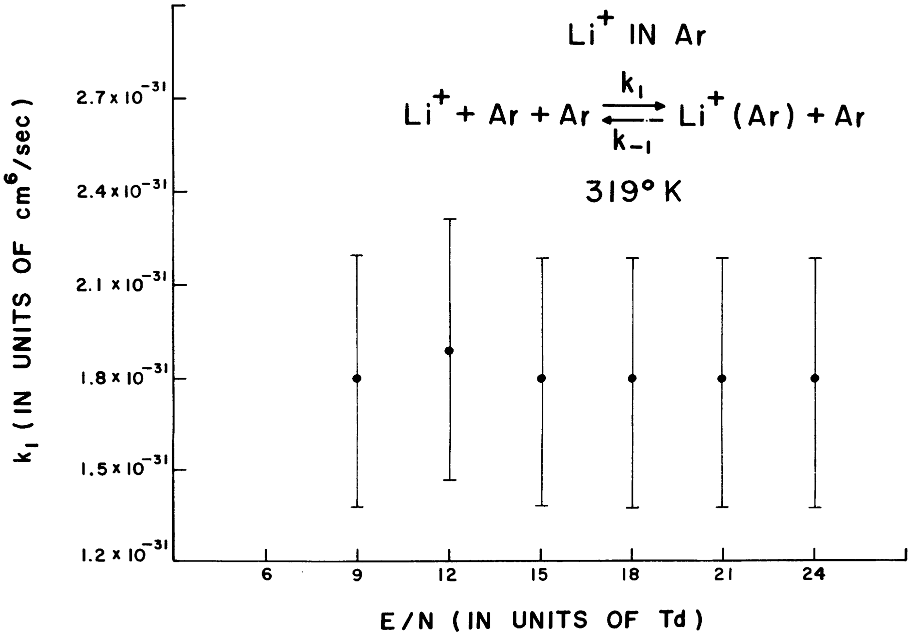

FIG. 10. Association-rate coefficient as a function of E/N.

of the drift distance, and ±1 μsec in determination of the time of drift.

For the mobilities of K^+ in N_2, K^+ in Ar, and Li^+ in Ar, the possible systematic errors were combined by the means of error propagation shown in Beers.[27] The contribution of random errors was determined from the scatter of the mobility determinations and combined with the systematic errors as independent errors. We arrived at the zero-field reduced mobility of K^+ in N_2 equal to 2.55 ± 0.06 $cm^2/V\,sec$, measured at 310 °K; that for K^+ in Ar equal to 2.73± 0.06 $cm^2/V\,sec$, measured at 310 °K; and that for Li^+ in Ar equal to 4.57±0.12 $cm^2/V\,sec$, measured at 319 °K. Each error indicated is the standard deviation of the value of the mobility. For comparison with "maximum possible" errors sometimes quoted in the literature, our standard deviations should be multiplied by a factor of 3.

The rate-coefficient determinations are subject to errors of at least two types. The first type is systematic error in the determination of the parameters, five measured and one deduced. We assessed the impact of systematic errors in the following fashion. Starting with measured and calculated profiles which were fit as well as possible, we changed the values of pressure, temperature, drift time, drift distance, drift voltage, and Li^+ mobility in the model by the maximum that they might be incorrectly determined and each in the direction which would yield the maximum change in the calculated profiles. We then refit the model to the measured data and obtained a new pair of rate coefficients. This procedure indicated that the most severe misdetermination of all these parameters could cause errors in the deduced association-rate coefficients of about ±16% and the deduced collisional-dissociation-rate coefficients of about ±10%. These percentages and the ones which follow allow for the fact that we fit to discrete values of the rate coefficients.

The second source of errors is associated with our inability to achieve a perfect fit to each of the measured profiles simultaneously. Therefore, after pairs of rate coefficients were determined, we also found the best pair of rate coefficients for *each* of the four individual profiles. We found that any of the curves could be well fit with modest changes in the rate coefficients. These exercises suggested that the need to compromise when fitting four profiles simultaneously, perhaps due to the assumption in the model of constant gas temperature over the whole drift range but also perhaps due to other inadequacies in the model or the data-gathering process, could introduce errors in the determination of the association-rate coefficients of about ±8% and in the determination of the collisional-dissociation-rate coefficients of about ±12%. The error bars in Figs. 10 and 11 reflect the sum of these two sources of possible errors, ±24% for

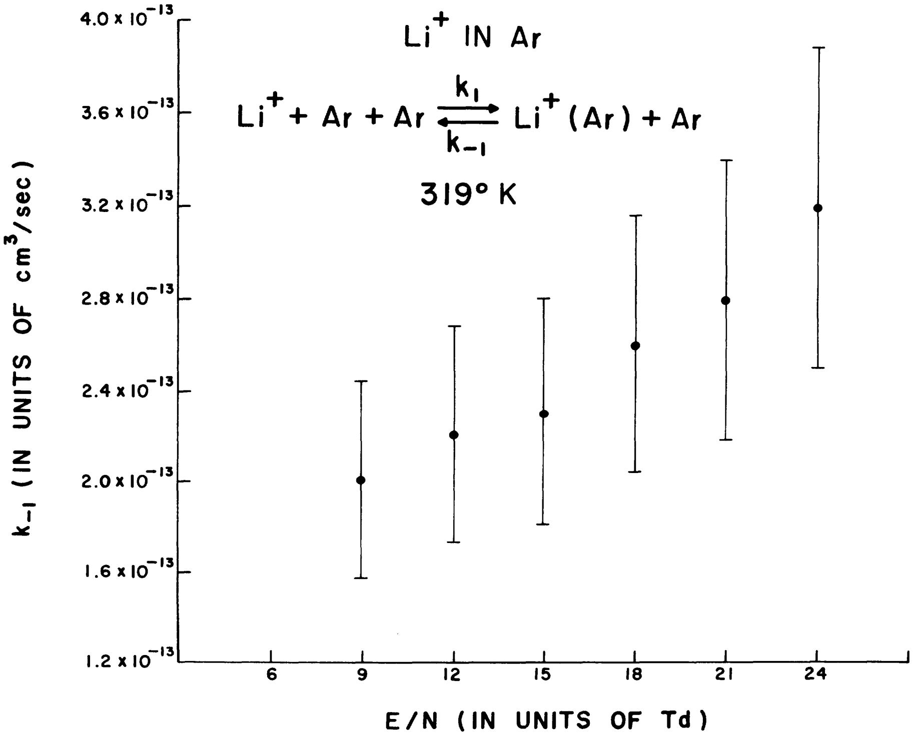

FIG. 11. Collisional-dissociation-rate coefficient as a function of *E/N*.

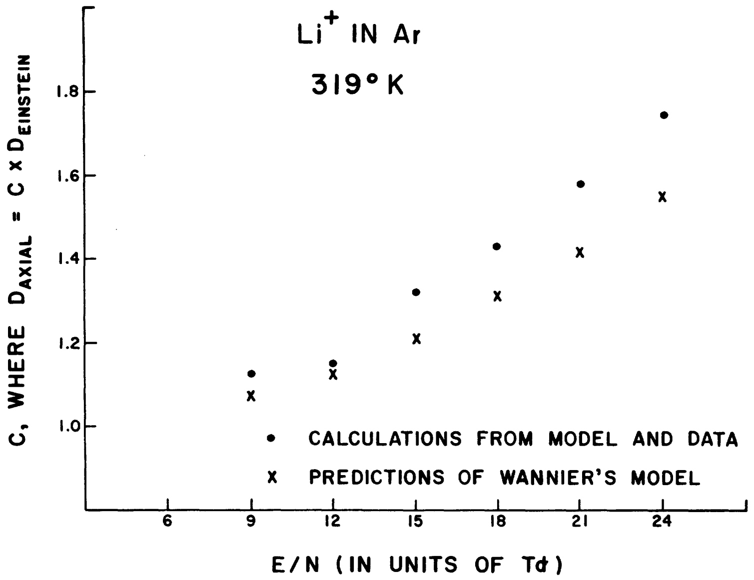

FIG. 12. Multiplicative factor by which axial diffusion coefficient exceeds value calculated from low-field mobility using Einstein equation. Comparison of factors deduced from experiment with factors calculated using Wannier's model.

the association-rate coefficients and ±22% for the collisional-dissociation-rate coefficients.

We have not found a satisfying method of establishing the error of the Li$^+$(Ar) mobility in Ar. We have conservatively chosen to assign to it about twice the percentage error of the "maximum possible" Li$^+$-in-Ar error, resulting in the zero-field reduced mobility of Li$^+$(Ar) in Ar being determined as 2.0± 0.3 cm^2/V sec at 319°K.

V. COMPARISONS AND CONCLUSIONS

Our measurement of the mobility of K$^+$ in N$_2$ at 2.55±0.06 cm^2/V sec at 310 °K is in excellent agreement with that of Moseley *et al.*,[4] who quote 2.55 cm^2/V sec at 300 °K, and with that of Crompton and Elford,[5] who quote 2.54 cm^2/V sec at 294 °K. Such agreement seems to justify the suggestion of McDaniel and Martin[28] that this mobility be used for pressure calibration in atomic collision experiments. Our measurement of the mobility of K$^+$ in Ar at 2.73±0.06 cm^2/V sec at 310 °K is in good agreement with a recent measurement of James *et al.*[29] who have obtained a value of 2.66 cm^2/V sec at 300 °K.

Munson and Tyndall[30] and Munson and Hoselitz[31] studied the drift of alkali ions through gases in 1939. We assume that they reduced their measured mobilities to 760 Torr but left them at 17 °C where the measurements were made. If we make the additional reduction to 0 °C, we find that our measurements are in good agreement with theirs. For K$^+$ in Ar, they measured 2.64 cm^2/V sec, while we have measured 2.73 cm^2/V sec. For Li$^+$ in Ar, they measured 4.7 cm^2/V sec, while we have measured 4.57 cm^2/V sec. When Li$^+$ drifted in Ar, they observed a cluster ion with a mobility of 1.97 cm^2/V sec. We have determined that the mobility of Li$^+$(Ar) in Ar is 2.0 cm^2/V sec, suggesting that Li$^+$(Ar) was the cluster ion in the older experiment of Munson and Hoselitz.

While there have been two other observations of clustering when Li$^+$ drifted in Ar,[31,26] we do not know of any other measurements of the rate coefficients for this system [reaction (1)]. It is interesting to take the rate coefficients deduced for our lowest E/N, $k_1 = 1.8\times10^{-31}$ cm^6/sec and $k_{-1} = 2.0\times10^{-13}$ cm^3/sec, and calculate the time constants associated with each process. At 1 Torr and 319 °K, the gas number density is 3×10^{16} molecules cm^{-3}, yielding a time constant for clustering of 6×10^{-3} sec. Similarly, the time constant for collisional dissociation is found to be 1.6×10^{-4} sec. Thus the time required for this reversible process [reaction (1)] to achieve chemical equilibrium is dominated by the time constant for dissociation of the cluster ion. At equilibrium, there would be about 3% Li$^+$(Ar) cluster ions and about 97% unclustered Li$^+$ ions.

ACKNOWLEDGMENTS

We wish to thank Dr. M. D. Kregel for his efforts in developing the model we used for our data reduction. We also wish to thank our past and present colleagues at the Ballistic Research Labs., Dr. F. E. Niles, Dr. J. M. Heimerl, Dr. L. J. Puckett, and Dr. W. C. Lineberger, for their wise counsel and profitable comments. Special thanks are due to D. G. McCoy for his technical assistance in the construction and maintenance of the equipment. We are indebted to Professor I. R. Gatland for suggestions concerning this manuscript.

*Present address: Dept. of Physics, University of Colorado, Boulder, Colo.

[1] R. S. Narcisi and A. D. Bailey, J. Geophys. Res. **70**, 3687 (1965).

[2] A. C. Aikin and R. A. Goldberg, J. Geophys. Res. **78**, 734 (1973).

[3] G. E. Keller and R. A. Beyer, J. Geophys. Res. **76**, 289 (1971).

[4] J. T. Moseley, I. R. Gatland, D. W. Martin, and E. W. McDaniel, Phys. Rev. **178**, 234 (1969).

[5] R. W. Crompton and M. T. Elford, Proc. Phys. Soc. Lond. **74**, 497 (1959).

[6] R. A. Beyer and G. E. Keller, Trans. Am. Geophys. Union **52**, 303 (1971).

[7] G. E. Keller and F. E. Niles, Chem. Phys. Lett. **10**, 526 (1971).

[8] K. G. Spears, J. Chem. Phys. **57**, 1850 (1972).

[9] G. E. Keller, M. R. Sullivan. L. M. Colonna-Romano, and M. D. Kregel, Ballistic Research Laboratories Report No. 1617, 1972 (unpublished). This report contains a complete FORTRAN listing of the Kregel model. The report can be obtained from either the National Technical Information Service, Springfield, Va. 22151 or the Defense Documentation Center, Cameron Station, Alexandria, Va. 22314. The cost is $3.00; refer to Report No. AD 907 581.

[10] S. B. Woo and J. H. Wealton, Phys. Rev. **180**, 314 (1969). See also S. B. Woo and J. H. Whealton, Phys. Rev. A **1**, 1558 (1970); and G. E. Keller, M. R. Sullivan, and M. D. Kregel, Phys. Rev. A **1**, 1556 (1970).

[11] J. H. Schummers, G. M. Thomson, D. R. James, E. Graham IV, I. R. Gatland, D. W. Martin, and E. W. McDaniel. Georgia Institute of Technology Technical Report, 1972 (unpublished). J. H. Schummers, G. M. Thomson, D. R. James, E. Graham IV, I. R. Gatland, and E. W. McDaniel, Phys. Rev. A 7, 689 (1973).

[12] L. G. H. Huxley, R. W. Crompton, and M. T. Elford, Br. J. Appl. Phys. **17**, 1237 (1966).

[13] We wish to thank Professor E. W. McDaniel and Professor D. W. Martin for their gifts of these materials.

[14] R. W. Crompton, M. T. Elford, and J. Gascoigne, Aust. J. Phys. **18**, 409 (1965).

[15] D. L. Albritton, T. M. Miller, D. W. Martin, and E. W. McDaniel, Phys. Rev. **171**, 94 (1968).

[16] L. J. Puckett, M. W. Teague, and D. G. McCoy, Rev. Sci. Instrum. **42**, 580 (1971).

[17] J. Heimerl, R. Johnsen, and M. A. Biondi, J. Chem. Phys. **51**, 5041 (1969).

[18] David Edelson, J. Appl. Phys. **39**, 3497 (1968).

[19] J. J. Lowke, Aust. J. Phys. **15**, 39 (1962).

[20] J. H. Whealton and S. B. Woo, J. Appl. Phys. **40**, 3060 (1969).

[21] M. D. Kregel (private communication).

[22] G. E. Keller and L. M. Colonna-Romano, Bull. Am. Phys. Soc. 18, 804, (1973).

[23] G. H. Wannier, Bell Syst. Tech. J. **32**, 170 (1953).

[24] E. W. McDaniel and J. T. Moseley, Phys. Rev. A **3**, 1040 (1971).

[25] G. M. Thomson, J. H. Schummers, D. R. James, E. Graham, I. R. Gatland, M. R. Flannery, and E. W. McDaniel J. Chem. Phys. **58**, 2402 (1973).

[26] L. G. McKnight and J. M. Sawina, Bull. Am. Phys. Soc. 18, 804 (1973).

[27] Yardley Beers, *Introduction to the Theory of Error*, 2nd ed. (Addison-Wesley, Reading, Mass., 1957), Sec. V.

[28] E. W. McDaniel and D. W. Martin, Rev. Sci. Instrum. **42**, 157 (1971).

[29] D. R. James, E. Graham, G. M. Thomson, I. R. Gatland, and E. W. McDaniel, Journal of Chemical Physics J. Chem. Phys. **58**, 3652 (1973).

[30] R. J. Munson and A. M. Tyndall, Proc. R. Soc. Edinb. A **172**, 28 (1939).

[31] R. J. Munson and K. Hoselitz, Proc. R. Soc. A172, 43 (1939).